Simulation and Optimization of Cyclone Dust Separators

Beate Breiderhoff, Thomas Bartz-Beielstein,
Boris Naujoks, Martin Zaefferer,
Andreas Fischbach, Oliver Flasch, Martina Friese,
Olaf Mersmann, Jörg Stork

Fakultät für Informatik und Ingenieurwissenschaften, FH Köln
Steinmüllerallee 1, 51643 Gummersbach
Tel.: +49 2261 8196-0
Fax: +49 2261 8196-15
E-Mail: {first-name}.{last-name}@fh-koeln.de

1 Introduction

The reduction of emissions from coal-fired power plants is a demanding task. Cyclone separators are frequently used devices for filtering the flue gas of such plants. They remove dispersed particles from gas. Their advantages are simple structure, low costs and ease of operation. Collection efficiency and pressure loss are the two most important performance parameters. They are heavily influenced by the choice of several geometrical design parameters, like height or diameter. This results into a Multi-Objective Optimization (MOO) problem, the so called Cyclone Optimization Problem (COP). This study shows how a COP can be solved and analyzed, based on an analytical, deterministic model. Furthermore, the analytical model is extended by adding several noise variables. These enable to evaluate robustness of solutions, and yield a better estimate of how noisy real-world circumstances affect the problem. Techniques like a classical as well as a model-supported SMS-EMOA are used to handle the MOO problem.

The remainder of the paper is structured as follows. Section 2 provides an overview on previous research and methods w.r.t. the modeling and the COP in particular as well as MOO. This section is followed by a short summary of the research questions and goals in Section 3. Section 4 describes the problem setup, introducing parameterizations for the COP. A sensitivity analysis of the problem is depicted in Section 5, which is followed by the description of the performed optimization experiments and their results in Section 6. A short summary and a discussion of the findings

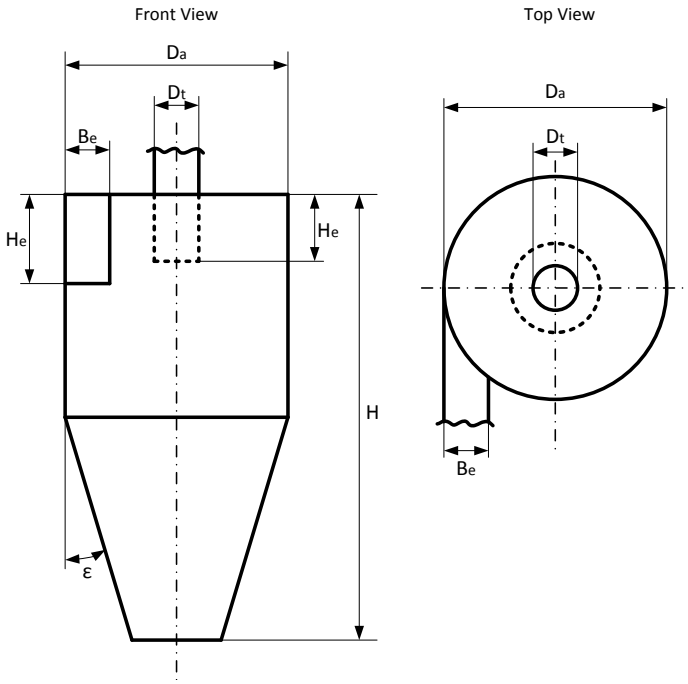

Figure 1: Schematic representation of a cyclone dust separator.

is given in Section 7. The paper closes with an outlook on future research in Section 8.

2 Previous Research and Methods

2.1 Cyclone Optimization

Cyclones exist in different shapes but the reverse flow cyclone represented in Fig. 1 is the most common design in industry. The principle of cyclone separation is simple: the gas-solid mixture enters at the top section tangentially. The cylindrical body induces a spinning, vortexed flow pattern to the gas-dustmixture. Centrifugal force separates the dust from the gas stream: the dust is moved to the walls of the cylinder and down the conical section to the dust outlet while the gas exits through the outlet pipe.

2.1.1 Significant parameters of a cyclone

Several characteristics constitute a COP.

1. Geometric shape
   Seven geometric parameters allow to describe the cyclone as shown in Fig. 1.

Table 1: Table of fluid, particle and geometrical parameters used in the experiments. Most values are taken from an example by Löffler [1].

	Parameter	Symbol	Default	Unit
Geometry	Cyclone diameter	D_a	1260	mm
	Cyclone height	H	2500	mm
	Outlet pipe diameter	D_t	420	mm
	Outlet pipe immersion	H_t	640	mm
	Cyclone cone angle	ϵ	13.134	$^\circ$
	Inlet height	H_e	600	mm
	Inlet width	B_e	200	mm
Fluid	Viscosity	μ	$18.5 \cdot 10^{-6}$	$Pa \cdot s$
	Flow Rate	V_p	5000	$\frac{m^3}{h}$
	Gas density	ρ_f	1.86	$\frac{kg}{l}$
Particle	Particle density	ρ_p	2	$\frac{kg}{l}$
	Particle concentration	c_e	50	$\frac{g}{m^3}$
Output	Pressure Loss	PL	2564	Pa
	Collection Efficiency	CE	0.89	(without unit)

2. Fluid/Gas properties
   Parameters like viscosity or density describe the carrier substance.
3. Particle Properties
   Density, concentration and distribution of particle sizes describe the particle composition.
4. Collection efficiency (CE)
   The overall CE of the cyclone describes the amount of particles filtered from the gas.
5. Pressure Loss (PL)
   The Pressure Loss is the difference in pressure between inlet and outlet.

These different characteristics are summarized in Table 1. Pressure loss and collection efficiency are the main criteria used to evaluate cyclone performance. Both are functions of the cyclone dimensions. Normally, the goal of cyclone design is to maximize collection efficiency and to minimize pressure loss by adjusting the geometric parameters.

2.1.2 Previous Optimization Studies

A first multi objective optimization of cyclone separators was performed by Ravi et al. [2]. They used the Non Dominated Sorting Genetic Algorithm NSGA II to optimize an analytical model by Mothes and Löffler [1], minimizing pressure loss and maximizing total collection efficiency for eight geometrical parameters. Elsayed and Lacor [3] optimized four geometrical parameters using computational fluid dynamics CFD models and the a model based on work by Barth [4]. They minimized pressure loss only, using the response surface methodology. Pishbin and Moghiman [5] optimized seven geometry parameters with a genetic algorithm, minimizing pressure loss and maximizing efficiency. They used a CFD model to construct the fitness function. The bi-objective problem was transferred to a single-objective problem using weights. Elsayed and Lacor [6] minimized pressure drop and cut-off diameter. They used a Pareto optimization approach, utilizing a Radial Basis Function Neural Network RBFNN. The RBFNN was trained with data from literature. A similar approach was taken by Safikhani et al. [7], where the data for trained neural network stemmed from CFD simulations.

The herein presented work uses the analytical model based on work by Barth [4] and Muschelknautz [8]. In contrast to previous approaches, we introduce a stochastic simulation based on the analytical model, where several parameters are assumed to be noisy. This allows to investigate robustness of solutions. Furthermore the more recent SMS-EMOA is used to solve the multi-objective COP. In case of the stochastic cyclone simulation, the model-free SMS-EMOA compared to a model-supported SMS-EMOA, using a Kriging surrogate model.

2.2 Analytical Models for Dust Separation

Barth [4] and Muschelknautz [8] proposed a simple model based on a force balance, as presented by Löffler [1]. This model enables to obtain the collection efficiency and pressure loss. The principle of calculation is based on the fact that a particle carried by the vortex is influenced by two forces: a centrifugal force and a flow resistance. They are expressed at the outlet pipe radius r_i where the highest tangential velocity occurs. The model represents a reverse flow cyclone with a tangential rectangular inlet. This is a simple and still useful model, by which friction was first introduced in cyclone modeling.

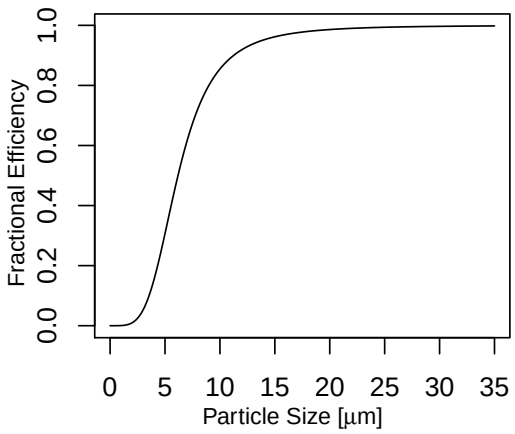

Figure 2: Fractional efficiency curve.

2.2.1 Collection Efficiency

The cyclone geometry, together with flow rate, defines the cut-size of the cyclone. Cut-size defines the particle size that will be collected with 50% efficiency. Smaller particles are collected with lower efficiency, larger with higher efficiency. Barth [4] developed a mathematical model for the cut-size as follows:

$$x_{Gr} = \sqrt{\frac{18\mu v_r r_i}{(\varrho_p - \varrho)v_{\phi i}^2}} \tag{1}$$

where r_i is the outlet pipe radius, v_r is the radial gas velocity on the outlet pipe and $v_{\phi i}$ is the cyclone inlet velocity.

The fractional efficiency curve assigns an efficiency to the particle diameter as shown in Fig. 2. Larger particles are collected more efficiently than smaller particles. The fractional efficiency curve is described by:

$$T(x) = \left(1 + \frac{2}{\frac{x}{x_{Gr}}^{3{,}564}}\right)^{-1.235} \tag{2}$$

where x is the particle size and x_{Gr} equals to Eq. (1). The overall collection efficiency is predicted according to:

$$E = \int_{x_{min}}^{x_{max}} T(x)q_e(x)dx = \sum_{x_{min}}^{x_{max}} T(\tilde{x_i})\Delta Q_e(x_i) \tag{3}$$

where x_{min} is the lower bound of the particle size, x_{max} is the upper bound of the particle size, $\tilde{x_i}$ is the mean particle size, $\Delta Q_e(x_i)$ is the change in distribution of particle sizes and $q_e(x) = \frac{\Delta Q_e(x_i)}{\Delta x_i}$.

2.2.2 Pressure Loss

Pressure loss is defined as the difference in pressure between two points of a fluid carrying body. It occurs with frictional forces. It relates directly to operation cost. Therefore an exact prediction is very important. Total pressure loss equals to:

$$\Delta p = \frac{\rho}{2} v_i^2 (\xi_{e-a} + \xi_{a-i} + \xi_{i-m}) \tag{4}$$

where ξ_{e-a} is the friction coefficient for the loss within the inlet (equals zero because of the tangential rectangular inlet) , ξ_{a-i} is the friction coefficient for the loss within the cyclone body, ξ_{i-m} is the friction coefficient for the loss within the outlet pipe and $\frac{\rho}{2} v_i^2$ is the relationship between pressure and velocity.

2.3 Model Alternatives

The above described analytical model is used as a predictor for collection efficiency and pressure loss. Several other analytical models of the cyclone separator exist [9]. Although all these methods have had a remarkable success, more advanced ideas are needed to model cyclones. Unsteadiness and asymmetry are for example two features not considered in classical cyclone theory that may affect the velocity distribution to a great extent, thus changing the model of the separation mechanism. On the other hand, as in many other fields, CFD currently emerges as a potentially accurate modeling technique.
Still, analytical models provide a good starting point for first investigations. Such models usually are not as precise as the more complex CFD models, but are much faster with respect to calculation time and other resources.

2.4 Multi Objective Optimization

In classical optimization methods only one objective is investigated. This is different in Multi Objective Optimization (MOO) where more than one objective can be optimized in parallel. However, new concepts had to be developed because these objectives are often conflicting, i.e. an improvement in one objective automatically leads to a deterioration in other objectives. Here, the concept of Pareto dominance comes into play. It says that

solution a dominates solution b if a is not worse in any objective and better than b in at least one objective. Formally, in case of minimization it reads

$$a \text{ dominates } b \Leftrightarrow \ \forall i: \ f_i(a) \leq f_i(b) \ \wedge \exists j: \ f_j(a) < f_j(b)$$

for a fitness function f of multiple objectives, $f(x) := (f_1(x), f_2(x), \dots)$ Based on this concept, an optimization process searches for solutions that are not dominated by any other solution. This results into a set of non-dominated solutions, called the Pareto front. The performance of an optimization process can therefore only be expressed in relation to a set of solution, rather than the quality of a single best solution.
Evolutionary Algorithms (EA) have become a standard tool for solving MOO problems. These algorithms are based on sets of solutions. This coincides well with the challenge of finding a set of solutions in MOO problems. Optimization Algorithms (EMOA) are modern MOO techniques that optimize the space that is covered by a Pareto front with respect to a predefined reference point. Maximizing this space, also called the hypervolume, pushes solutions more and more towards the desired objective values. Moreover, the hypervolume rewards a high diversity of solutions, i.e. a wide spread, and a smooth distribution of solutions along the border to the non-dominated area. All these properties are highly appreciated in MOO. One of the techniques employing hypervolume maximization is the SMS-EMOA (cf. Beume et al. [10]), which is also employed here.

2.5 Expensive Optimization Problems

In general, industrial design tasks can not be optimized by manufacturing multiple design instances and deciding for the best alternative afterwards. In almost all cases, this procedure would simply be too expensive. As a consequence, models are considered to estimate the performance of different designs before the actual manufacturing process. These simulations or models themselves can become time-consuming to evaluate. Developing surrogate approaches is the most important solution to that issue. In such approaches, the optimization problem (e.g. the cyclone model) is replaced by a cheaper, or easier to optimize surrogate model. A comprehensive survey of surrogate modeling in optimization was provided by Jin [11].
A methodical framework for surrogate model based optimization of noisy and deterministic problems is Sequential Parameter Optimization (SPO) introduced by Bartz-Beielstein et al. [12]. SPO has been developed for solving expensive algorithm tuning problems but can be directly employed for solving real world engineering problems as well.

One of the most often used surrogate-models is Kriging. This is partly due to the fact that it poses an excellent predictor of smooth, continuous problem landscapes. Moreover, it provides an uncertainty estimate of its own prediction, which can be used to calculate the Expected Improvement (EI) of a solution. This was used in Efficient Global Optimization by Jones et al. [13] to balance exploitation and exploration in the optimization process. In MOO, several approaches employ surrogate modeling. An overview of surrogate modeling in MCO is given by Knowles and Nakayama [14]. EGO has also been extended for MOO problems, as in the ParEGO Algorithm by Knowles [15] or the SMS-EGO approach suggested by Ponweiser et al. [16]. Emmerich et al. [17] show how the EI in hypervolume can be calculated exactly.

3 Questions and Goals

Real-world industrial multi-objective test cases are highly appreciated by the MOO research community because these allow for a comparison of methods apart from artificial test cases. The latter are usually used in the community but do not yield the complexity or significance of real-world applications. The COP is presented as a MOO test case and first results are presented. Moreover, the MOO results are compared to results from a single objective optimization approach to determine a possible lack of performance due to involving multiple objectives in parallel. Therefore, the single objective optimization results are compared to the extreme Pareto non-dominant solutions.
The cyclone model assumes a certain distribution of particle sizes as well as fixed, undisturbed settings of all other relevant variables. In practice, variables like the inflow speed or particle sizes will be noisy. That noise can be simulated by repeated sampling from random distributions, each sample leading to a new evaluation of the cyclone model. The repeated evaluation with different samples leads to a more time consuming target function for the optimization algorithm. To alleviate this issue, surrogate models can be introduced to support the optimization process. Therefore, the goals of this study are to:

- test the deterministic COP as a MOO problem.
- compare a single-objective and a multi-objective approach.
- analyze the influence of noise on the solution quality.
- determine influence of geometry, fluid and particle parameters.
- compare a model-free and a model-supported SMS-EMOA in case of optimizing a stochastic cyclone simulation.

Table 2: Particle size distribution table. Values are derived from an example presented by Löffler [1].

Intervall $[\mu m]$	Mean $[\mu m]$	Density	Cumulative
0-2	1	0	0
2-4	3	0.02	0.02
4-6	5	0.03	0.05
6-8	7	0.05	0.1
8-10	9	0.1	0.2
10-14	12.5	0.3	0.5
15-20	17.5	0.3	0.8
20-30	25	0.2	**1**

4 Problem Setup

4.1 Parameters of the Deterministic Cyclone Model

The herein described experiments are based on an example by Löffler [1]. This example uses the geometrical, fluid-specific, and particle-specific parameters summarized in Table 1. The geometrical parameters to be optimized are varied in fixed boundaries, which are ± 10 % of the default values from Table 1. Geometrical parameters could be varied in a much wider range, however, this range would not necessarily be fitting to the given fluid and particle parameters. Therefore, the 10% deviation was chosen as a typical experimental setup. A two-dimensional case (with D_a and H only) as well as a seven dimensional case with all seven parameters are investigated.

4.2 Stochastic Cyclone Simulation

In addition to the parameters from the deterministic model, three noise sources are introduced. That is, flow rate V_p, particle density ρ_p, and the particle sizes x_i used in the collection efficiency calculation can be subject to noise. The flow rate is allowed to vary in between $\pm 10\%$ of the default value, while particle density varies within $\pm 5\%$. In both cases, a uniform distribution is used. For the collection efficiency calculation, one sample is drawn in each of the intervals from Table 2, instead of simply using the midst of each interval. That is, the particle size in each interval is determined randomly with a uniform distribution. These values are then inserted in Eq. (3), to calculate the overall collection efficiency.

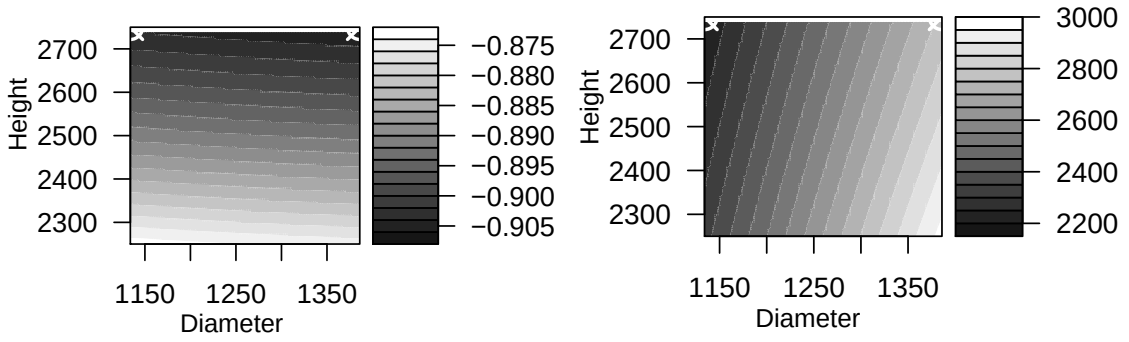

Figure 3: Surface of the deterministic objectives landscape. CE is left, PL is right. The Pareto set resides as white dots on the upper boundary of the plot. The extreme points (found by single objective optimization) reside in the upper corners. CE is negative, since all objectives are minimized.

5 Search-Space and Sensitivity Analysis

5.1 Deterministic Cyclone model

The objective landscape of the two-dimensional decision space is depicted in Fig. 3. The surface of the landscape is plotted based on a 100×100 point grid. Based on this sweep, the following classical analysis was performed.

1. Model fitting: for each objective, a regression model was fitted separately.
2. Desirability: define desirability for each objective.
3. Optimization: maximize the overall desirability.

The model fitting step involves the standard techniques from regression analysis, i.e., model specification, stepwise regression, and validation (considering residual plots etc.). The definition of desirability is elementary in this case: we defined a linear desirability function, which maps the interval of the CE and PL values to the intervals from zero to one. Since we are considering a minimization problem, the maximum CE and PL values are mapped to zero, whereas their minimum counterparts are mapped to one. Using classical optimization techniques, the geometrical mean of the two desirabilities is maximized. The following setting is considered optimal: $D_a = 1134, H = 2750, D_t = 462, H_t = 640, \epsilon = 13.13, H_e = 659$, and $B_e = 219$. The outlet pipe immersion H_t and the cyclone cone angle ϵ are set to their default values, because the analysis reveals that their effects are negligible. The classical approach results in a pressure loss value of $PL = 1385.35$ and a collection efficiency of $CE = -0.88$. The design based on the default values has an associated hypervolume of 2172.28, whereas the hypervolume, which is based on the desirability analysis is

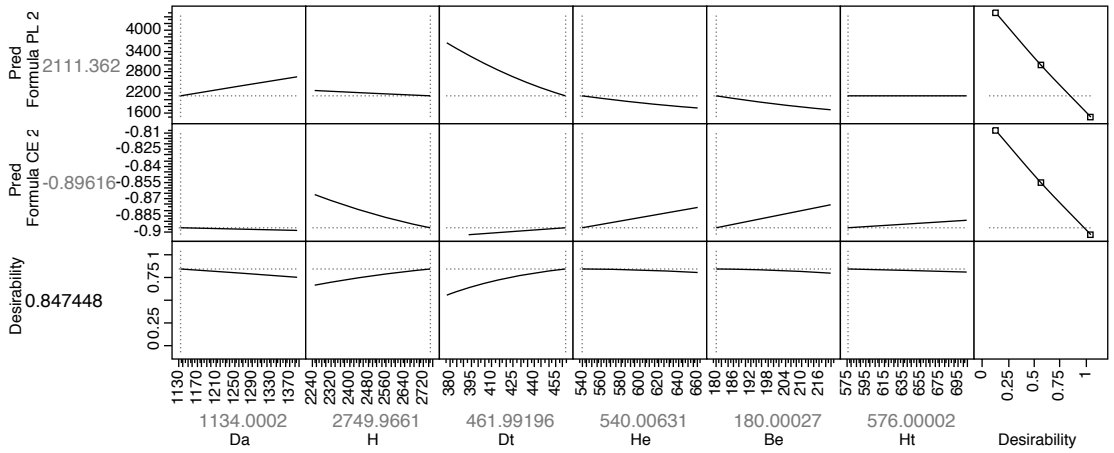

Figure 4: Search-space analysis of the deterministic landscape

3189.60. The reference point for the hypervolume calculation is 5000 PL and 0 CE. Before presenting a comparison of these rather simple results with state-of-art optimization techniques in Sect. 6, a sensitivity analysis of the stochastic cyclone simulation is presented in Sect. 5.2.

5.2 Stochastic Cyclone Simulation

First experiments where only D_a and H were varied showed that the noise level is high enough to make it hard to identify any structure in the problem landscape. Further experiments with repeated evaluations showed that structure seen in the deterministic model resurfaces for the expected value. The introduced noise is multiplicative, both for CE and PL. Variance is lowest for solutions with good CE and PL values.
The sensitivity analysis of the stochastic simulation is based on 100,000 data points, that were generated via Latin Hypercube Sampling (LHS). Each design point was evaluated ten times. The LHS intervals were determined as default value $\pm 10\%$. Default values were introduced in Table 1. Based on these modifications of seven geometrical parameters, the simulated output values are obtained, namely pressure loss and collection efficiency. Since both output values are minimized, CE has to receive a negative sign. Noise variables, i.e., flow rate V_p, particle density ρ_p, and particle sizes x_i were added to the analysis.
The distribution of the CE variable has a long tail, see Fig. 5. Values from the upper ten percent quantile are labeled. The histograms shown that V_p has no effect on CE, whereas ρ_p has a significant impact:

- Small ρ_p values result in worse CE, and vice versa.

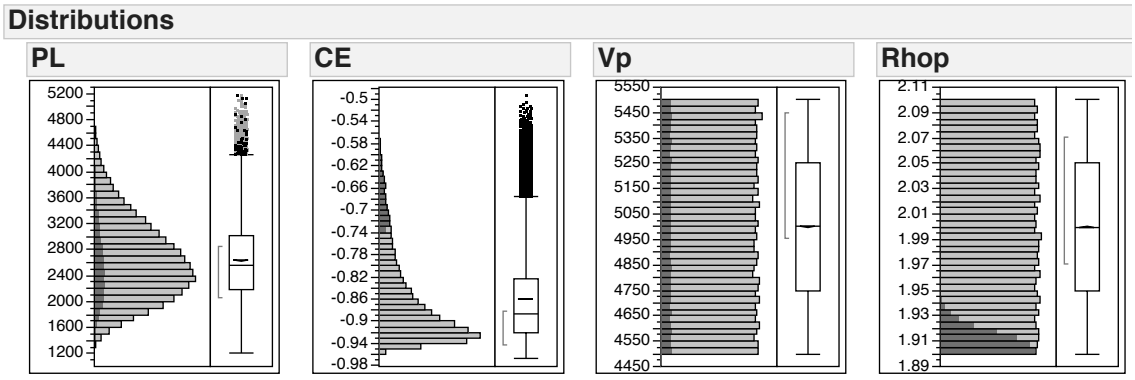

Figure 5: Distribution analysis.

Furthermore, we can conclude that CE is dominated by the noise factor ρ_p. This can be seen from the regression tree analysis, which was performed to discover the driving forces. This simple analysis, visualized in Fig. 6, reveals that

- regarding collection efficiency, about two-third of the variance can be explained by the noise variable particle density ρ_p
- regarding pressure loss, it can be seen that a large amount of the variance can be explained by the outlet pipe diameter D_t and the noise variable particle density ρ_p.

As can be seen, V_p is the only noise variable that has influence on PL, which is to be expected because it is the only of the three sources to be related to PL in the model formulas. V_p is also the only noise source that does not influence CE. For CE, ρ_p has the strongest influence. Figure 7 illustrates the effects of the design variables on PL. Fig. 8 shows the results from a sensitivity analysis, which is based on a regression model. Only a model for PL could be obtained, because CE is determined by the noise variable ρ_p. Best configurations used settings at the border of the region of interest. The expected pressure loss of this setting is 1353.95 .

6 Optimization

6.1 Optimization of the Deterministic Cyclone Simulation

6.1.1 Setup

Two optimization-cases are tested:
Two-dimensional case: For a first impression, only two parameters are va-

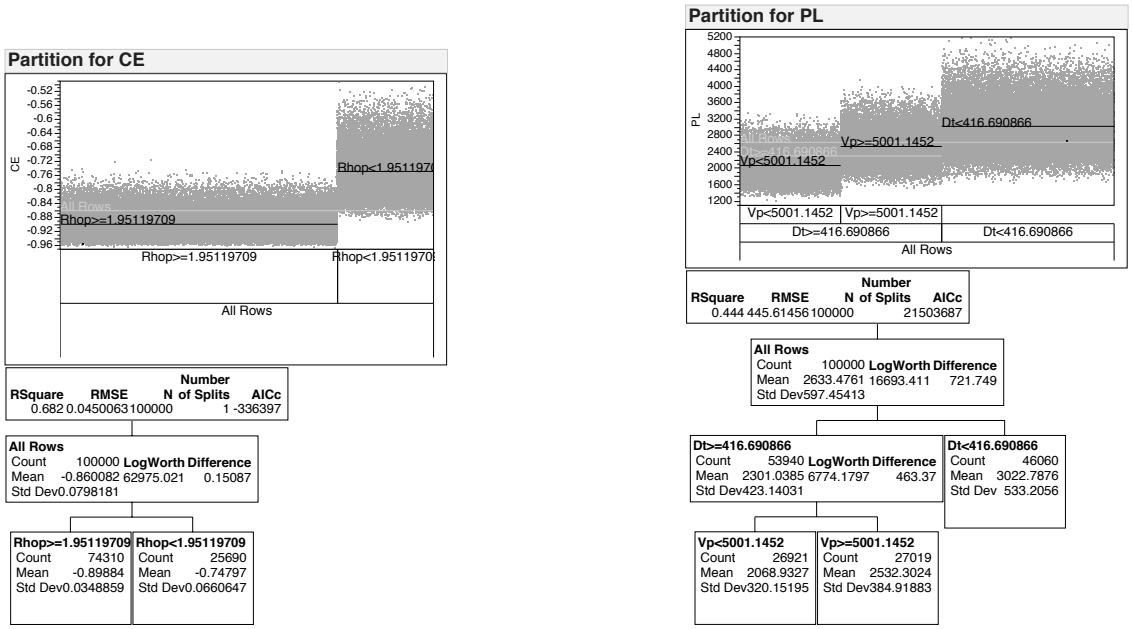

Figure 6: Regression tree analysis. *Left:* Collection efficiency: one single split explains 68 % of the variance in the data. *Right:*Pressure loss: the two splits explain 44% of the variance in the data.

Sorted Parameter Estimates

Term	Estimate	Std Error	t Ratio	Prob>|t|
Dt	-0.006459	1.514e-5	-426.5	<.0001*
Da	0.0009369	5.048e-6	185.59	<.0001*
Be	-0.005612	3.18e-5	-176.5	<.0001*
He	-0.001693	1.06e-5	-159.7	<.0001*
H	-0.000132	2.544e-6	-51.73	<.0001*
(Da-1260)*(Dt-420)	7.4058e-7	2.079e-7	3.56	0.0004*

Figure 7: The outlet pipe diameter D_t has the greatest impact on pressure loss.

ried, the cyclones diameter and height. All other parameters are kept constant at their default value. Both pressure loss (PL) and collection efficiency (CE) are optimized by a simple steady-state SMS-EMOA (cf. Beume et al. [10]), with a population size of 100. The employed implementation of the SMS-EMOA is part of the *SPOT* R-package[1]. As a comparison, the single objective Nelder-Mead [18] algorithm for box-constrained [19] problems is used to optimize both objectives separately. The SMS-EMOA receives a function evaluation budget of 100,000. The Nelder-Mead algorithm receives the same budget, but is expected to converge in a small fraction of that budget.

Seven-dimensional case: The complete set of seven geometrical parameters is optimized in the same way. Due to the larger search space dimen-

[1]SPOT is available at `www.cran.r-project.org/package=SPOT`

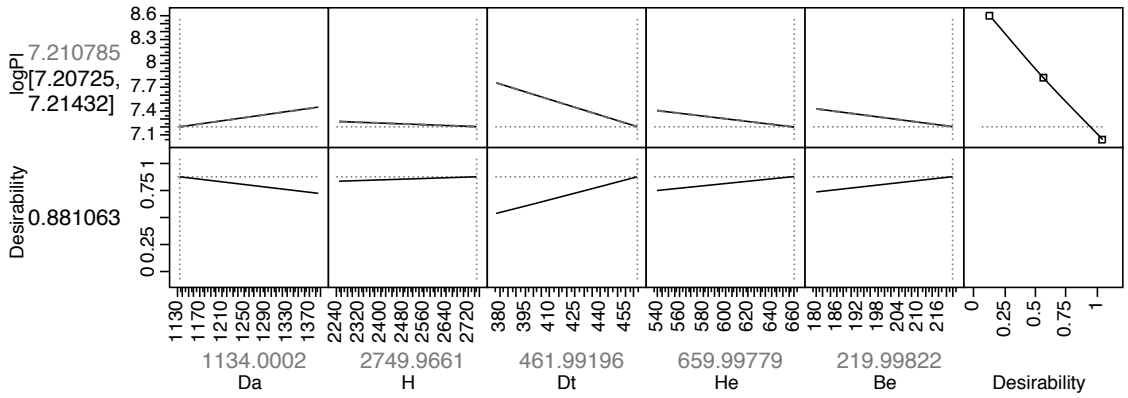

Figure 8: Prediction profile. The desirability of the objective PL is maximized if the values of the input variables as shown above are selected. Note, best configurations used settings at the border of the regions of interest.

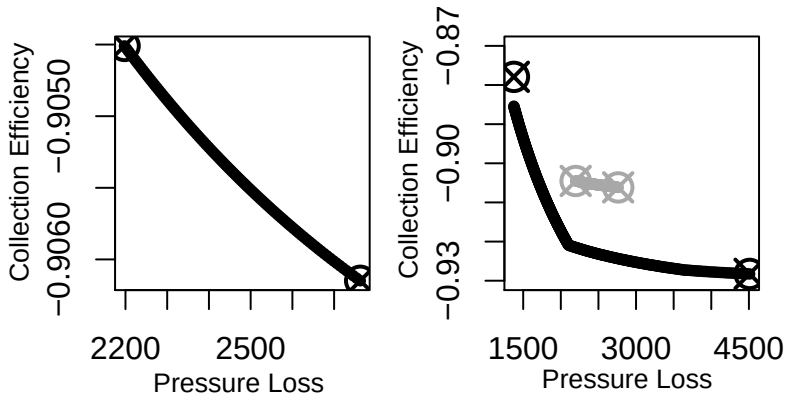

Figure 9: Pareto front (black dots) estimated by SMS-EMOA for the deterministic, bi-objective problem. Crossed circles show the results of the single objective Nelder-Mead optimizer. Left: two-dimensional case, only diameter and height are optimized. Right: Optimization of all seven geometrical parameters. The grey dots on the right side show, again, the two-dimensional case front.

sion, both the function evaluation budget and the population size of the SMS-EMOA were multiplied by a factor of 3.5.
These first and very simple optimization experiments are not repeated but simply run once, to give a first impression of the found Pareto fronts.

6.1.2 Results from the Deterministic Optimization Runs

The results of the first optimization experiments is depicted in Fig. 9. From the results of the optimization, and the shape of the two-dimensional objective landscape shown in Fig. 3, it is clear that the true Pareto front resides on the upper boundary of the cyclone height. That is, when the height is chosen to be maximal any value of the diameter leads to Pareto optimal

solutions.
In the two-dimensional case, the hypervolume of the Pareto front estimate is 2539, whereas in the seven-dimensional case 3341 is reached. This is based on the same reference point with 5000 PL and 0 CE as used in Section 5.1. The Pareto fronts of the two-dimensional and seven-dimensional decision space lead to different Pareto front shapes. The former is continuous, whereas the latter seems to have a discontinuity at the knee of the front. The larger search space of the seven-dimensional problem allows to find better solutions, which all dominate solutions found for the two-dimensional case. Furthermore, the single objective optima reside on the extreme points of the two-dimensional decision space front. In case of the seven-dimensional decision space, the optimum found by Nelder-Mead for the PL is separate from the corresponding extreme point. While both have nearly identical PL values, the collection efficiency is much worse for the single objective optimizer.
A scatter-plot analysis reveals that the ϵ parameter shows the least structure, thus having little influence on solution qualities. Many of the Pareto optimal points reside on the boundaries of several parameters. The discontinuity in the Pareto front seems to be caused by certain Parameters (e.g. B_e, H_e or D_t) hitting a boundary.

6.2 Optimization of the Stochastic Cyclone Simulation

6.2.1 Setup

In this optimization study, a model-free SMS-EMOA as well as a surrogate model supported SMS-EMOA are compared. A fixed budget of 1 million function evaluations is given for each model-free SMS-EMOA run. The budget is 10 times larger than the budget used in the deterministic example, due to the difficulties created by the high noise level. Results are compared for 1, 10, 100 and 1000 evaluations of each individual. Larger numbers of repeated evaluations lead to a corresponding decrease in the number of generations. Mean values of these repeated evaluations are used as approximations of the true fitness. With these settings, each SMS-EMOA run takes approximately 210 seconds[2].
The Sequential Parameter Optimization Toolbox (SPOT) is used for the model-supported run. The chosen model type is Kriging. The Kriging implementation is based on work by Forrester et al. [20]. Since Kriging is

[2]The experiments, including runtime estimation, have been performed on a System with 3.40 GHz Intel Core i5, 8GB RAM, Windows 64.

expensive to build, the model should not be build too often. This is especially true for this study, since the target function is not very expensive. Therefore, the initial design (or population) of the model-supported run is chosen to contain 35 points, that is 5 for each decision space dimension. Each point is simulated 1000 times. More complex noise handling (e.g., Multi-Objective Optimal Computing Budget Allocation MOCBA [21] or similar approaches) are not employed here since only one surrogate optimization step is performed. That means, the Kriging model is trained only once. The SMS-EMOA is employed to optimize the surrogate model. It receives a budget of 77,000 evaluations of the Kriging surrogate, thus finding a 100 point Pareto front estimation. No EI criterion is employed, since the harsh time restriction makes pure exploitation the more desirable choice. This result into a run-time of roughly 210 seconds, consistent with the model-free run-time. Here, the main contributors to run-time are the training of the Kriging model, and the subsequent optimization on the Kriging model.
Both the SMS-EMOA and the Kriging-supported SMS-EMOA are run 20 times. The quality of each point in the resulting Pareto front estimates are validated by 10,000 runs of the stochastic simulation. To compare, the hypervolume indicator is used with a reference point of 5000 PL and zero CE.

6.2.2 Results from Stochastic Optimization Runs

The optimization results are summarized in Fig. 10. For the model-free SMS-EMOA, increasing the number of evaluations per point seems to yield no improvement. Exploring more points is at least as profitable as estimating the quality of each point more accurately. Still, it can be seen, that the model supported SMS-EMOA clearly outperforms the model-free SMS-EMOA. This is despite of the fact, that the model uses a much smaller budget than the SMS-EMOA. The run-time of both approaches is about equal. The Kriging model seems to deal well with the remaining noise in the objective function, yielding a more easy to optimize surrogate. This is especially interesting since the target-function is not exactly expensive, which would be the usual case where Kriging surrogates work well. Still, 1000 evaluations of each point make this a semi-expensive problem. One explanation for the excellent performance of the model-based SMS-EMOA, besides its ability to smoothen the noisy landscape, may be, that even in the seven-dimensional case, the true front is spread along several boundaries of the decision space. This could already be observed for the

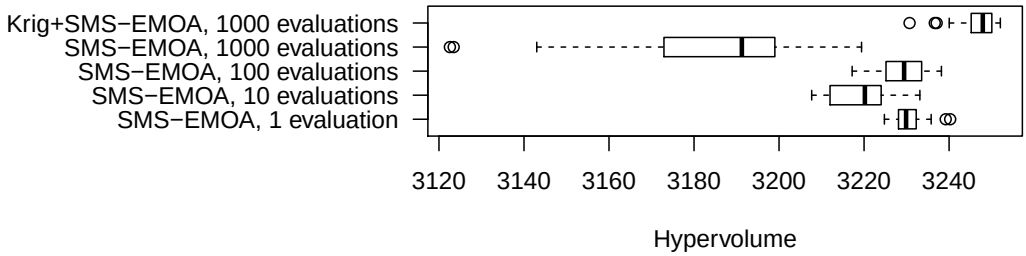

Figure 10: Boxplots for the optimization experiments with the stochastic simulation. The x-axis shows hypervolume of the estimated fronts, validated by 10,000 runs for each point. Higher values are better. Evaluation numbers refer to the repeated evaluation of each point.

deterministic model, and holds here as well. That may lead to a situation, where the surrogate model does not have to have high accuracy over the whole search space because it suffices to predict decreasing values towards the boundaries.

7 Summary and Discussion

This paper presents a multi objective optimization problem, based on a deterministic, analytical model of a cyclone dust separator. Noise influence was added, thus generating a stochastic simulation model. This allowed not only to optimize, but also to investigate robustness of solutions, against uncertainty in the noisy variables.

In case of the deterministic model, users can choose preferable results from the Pareto front, depending on their preference of CE and PL combinations. Preferred design points can be further analyzed with the stochastic simulation model. For instance, a user might choose the knee of the Pareto front (see right plot in Fig. 9) and an extreme point on the upper left part of the Pareto front, as summarized in Table 3. Those settings could be reevaluated with the stochastic model, yielding resulting variance estimates as depicted in Fig. 11. In practice, it may occur, that a user would prefer the extreme solution. While this solution has a worse expected value for CE, there is strong overlap between both solutions. On the other hand, the PL values show clearly a significant difference, thus leading to the potential preference of the extreme point.

It was also shown, that the stochastic simulation can be optimized directly. While the high noise level makes this more costly for a simple SMS-EMOA, a surrogate model based approach seems to handle the issue more efficiently.

The classical, single objective Nelder-Mead is able to identify the optima

Table 3: Two Points from the Pareto front found by SMS-EMOA on the deterministic model, with all seven geometrical parameters considered. The whole front is shown in Fig. 9 on the right.

Parameter	Point 1 (knee)	Point 2 (extreme)
D_a	1134	1134
H	2750	2750
D_t	462	462
H_t	576	576
ϵ	13.92	12.81
H_e	540	660
B_e	180	220
PL	2103.87	1375.90
CE	-0.921	-0.86

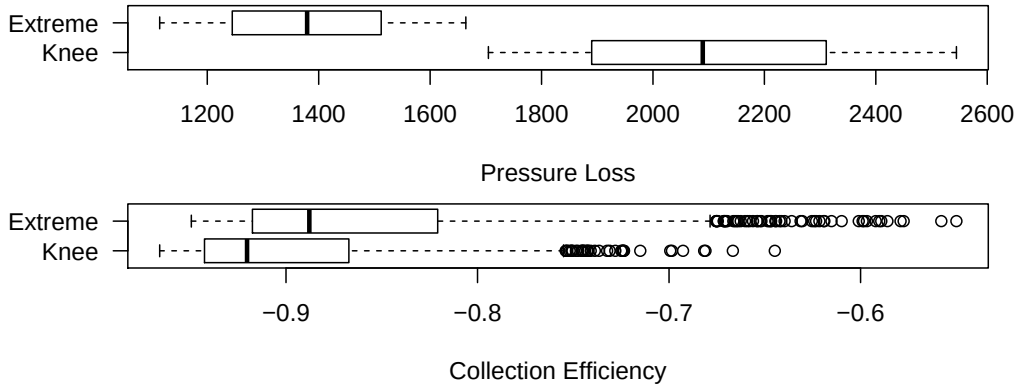

Figure 11: Boxplots for the knee, and an extreme point of the Pareto front found for the deterministic model. Corresponding to the parameters in Table 3, reevaluated 1000 times with the stochastic simulation. Lower values are better.

of the deterministic objective, but fails in case of the noisy simulation.
The presented cyclone model representations are of comparativly simple structure, and thus are good candidates for real-world based multi objective test problems.

8 Outlook

While the analytical cyclone model does pose an interesting MOO problem, it lacks any information about quality of non-standard problems and solutions. That means, whenever particle, fluid or geometry attributes stray to far from the standard, the models quality deteriorates. For instance, the model is unable to represent non-centric positions of the outlet or slanted

inlets. Still, such changes to geometry are of high interest to practitioners in industry. To get a better quality estimate of these geometries, CFD models are used.
CFD models offer a wide variety to model the dynamics of particles in any kind of flow. However, such models need different preliminaries like the discretization of the considered space (meshing) and a solver for the resulting set of (partial) differential equations. This results in rather time-consuming and thus expensive simulations for each design alternative. However, such simulations can be very precise, mapping the real process with a very high accuracy and thus might be worth the effort.
To support the optimization of such time consuming simulations, the analytical model may still be of use. It can be used for multi-fidelity optimization of such CFD models, using techniques like Co-Kriging [20]. While they represent only a part of the possible number of geometrical parameters, they can still be used to improve the quality of such a Co-Kriging model, which would otherwise have to rely on accurate, but sparse, CFD simulations only. Furthermore, the optima or Pareto fronts found on the analytical model can be used to generate starting points for the optimization of the more complex CFD models.

Acknowledgements

This work has been partially supported by the Federal Ministry of Education and Research (BMBF) under the grants MCIOP (FKZ 17N0311) and CIMO (FKZ 17002X11).

References

[1] Löffler, F.: *Staubabscheiden*. Lehrbuchreihe Chemieingenieurwesen, Verfahrenstechnik. Thieme. ISBN 9783137122012. 1988.

[2] Ravi, G.; Gupta, S. K.; Ray, M. B.: Multiobjective Optimization of Cyclone Separators Using Genetic Algorithm. *Industrial & Engineering Chemistry Research* 39 (2000) 11, S. 4272–4286.

[3] Elsayed, K.; Lacor, C.: Optimization of the cyclone separator geometry for minimum pressure drop using mathematical models and {CFD} simulations. *Chemical Engineering Science* 65 (2010) 22, S. 6048 – 6058.

[4] Barth, W.: Berechnung und Auslegung von Zyklonabscheidern auf Grund neuerer Untersuchungen. *Brennstoff-Wärme-Kraft* 8 (1956) 1, S. 1–9.

[5] Pishbin, S. I.; Moghiman, M.: Optimization of Cyclone Separators Using Genetic Algorithm. *International Review of Chemical Engineering* 2 (2010) 6, S. 683–691.

[6] Elsayed, K.; Lacor, C.: Modeling and Pareto optimization of gas cyclone separator performance using {RBF} type artificial neural networks and genetic algorithms. *Powder Technology* 217 (2012) 0, S. 84 – 99.

[7] Safikhani, H.; Hajiloo, A.; Ranjbar, M.: Modeling and multi-objective optimization of cyclone separators using {CFD} and genetic algorithms. *Computers & Chemical Engineering* 35 (2011) 6, S. 1064 – 1071.

[8] Muschelknautz, E.: *Vt-Hochschulkurs 2 [zwei], mechanische Verfahrenstechnik*. Verfahrenstechnik international ; Sonderh. Krausskopf. 1972.

[9] Cortes, C. Gil, A.: Modeling the gas and particle flow inside cyclone seperators. *Progress in Energy and Combustion Science* 33 (2007), S. 409–452.

[10] Beume, N.; Naujoks, B.; Emmerich, M.: SMS-EMOA: Multiobjective selection based on dominated hypervolume. *European Journal of Operational Research* 181 (2007) 3, S. 1653–1669.

[11] Jin, Y.: A comprehensive survey of fitness approximation in evolutionary computation. *Soft Computing* 9 (2005) 1, S. 3–12.

[12] Bartz-Beielstein, T.; Parsopoulos, K. E.; Vrahatis, M. N.: Design and analysis of optimization algorithms using computational statistics. *Applied Numerical Analysis and Computational Mathematics (ANACM)* 1 (2004) 2, S. 413–433.

[13] Jones, D.; Schonlau, M.; Welch, W.: Efficient Global Optimization of Expensive Black-Box Functions. *Journal of Global Optimization* 13 (1998), S. 455–492.

[14] Knowles, J. D.; Nakayama, H.: Meta-Modeling in Multiobjective Optimization. In: *Multiobjective Optimization*, S. 245–284. Springer. 2008.

[15] Knowles, J.: ParEGO: A hybrid algorithm with on-line landscape approximation for expensive multiobjective optimization problems. *IEEE Transactions on Evolutionary Computation* 10 (2006) 1, S. 50–66.

[16] Ponweiser, W.; Wagner, T.; Biermann, D.; Vincze, M.: Multiobjective Optimization on a Limited Budget of Evaluations Using Model-Assisted -Metric Selection. In: *PPSN*, S. 784–794. 2008.

[17] Emmerich, M.; Deutz, A.; Klinkenberg, J.: Hypervolume-based expected improvement: Monotonicity properties and exact computation. In: *Evolutionary Computation (CEC), 2011 IEEE Congress on*, S. 2147–2154. IEEE. 2011.

[18] Nelder, J. A.; Mead, R.: A Simplex Method for Function Minimization. *The Computer Journal* 7 (1965) 4, S. 308–313.

[19] Box, M. J.: A New Method of Constrained Optimization and a Comparison With Other Methods. *The Computer Journal* 8 (1965) 1, S. 42–52.

[20] Forrester, A.; Sobester, A.; Keane, A.: *Engineering Design via Surrogate Modelling*. Wiley. 2008.

[21] Lee, L. H.; Chew, E. P.; Teng, S.; Goldsman, D.: Optimal computing budget allocation for multi-objective simulation models. In: *Simulation Conference, 2004. Proceedings of the 2004 Winter*, Bd. 1, S. –594. 2004.